

Stress Response to Surface Alloying and Dealloying during Underpotential Deposition of Pb on (111)-Textured Au

J. W. Shin,* U. Bertocci, and G. R. Stafford

Materials Science and Engineering Laboratory, National Institute of Standards and Technology, Gaithersburg, Maryland 20899

Received: January 13, 2010; Revised Manuscript Received: March 12, 2010

The stress response during Pb underpotential deposition on (111)-textured Au has been examined on a cantilever beam electrode in perchloric acid supporting electrolyte. We observe a sweep rate dependence for both the individual voltammetric waves and the stress response that we attribute to kinetically controlled surface alloying [$(\sqrt{3} \times \sqrt{3}) R30^\circ$], which occurs only at low coverage. At high coverage, a hexagonal close-packed (hcp) Pb monolayer is formed while the surface alloy is removed. The stress hump that is coincident with the last voltammetric wave appears to be caused by the formation and removal of the surface alloy. Long-term potentiostatic pulsing experiments show slow stress changes during both the formation and the stripping steps, but only for the incomplete adlayer, confirming slow alloy and dealloy processes at those coverages. The voltammetry and surface stress after extended polarization at potentials where dealloying occurs show that the stable alloy structure and the hcp adlayer coexist and that the relative amounts of these phases are potential-dependent.

Introduction

The underpotential deposition (upd) of Pb on Au(111) has been studied extensively because of the enhanced catalytic activity for oxygen reduction at submonolayer coverage and to gain a better understanding of the earliest stages of metal electrodeposition.^{1–7} It has been reported that Pb forms hexagonal close-packed (hcp) islands at low coverage and an incommensurate hcp adlayer at full coverage. This is followed by electrocompression and rotation of the Pb adlayer as the potential approaches the equilibrium potential of bulk deposition.^{8–11} In our previous study,¹² we reported on the stress evolution during Pb upd. In the compression region, we were able to obtain the biaxial modulus of the Pb monolayer on (111)-textured Au by converting our stress-potential data into stress–strain, making use of Toney et al.'s near-neighbor distance data.¹¹ Interestingly, the modulus of the monolayer is close to that for Pb(111) in the bulk. In addition, a sudden and temporary change in the surface stress in the tensile direction (stress relaxation hump) was observed near the principal Pb upd peak (at ca. -0.65 V vs saturated Hg sulfate reference electrode (SSE)) and was attributed to the tensile stress induced by the coalescence of Pb islands. Seo et al.¹³ and Friesen et al.¹⁴ observed similar stress behavior during Pb upd on Au(111), but they related the stress relaxation hump to the rotation of the Pb adlayer, as reported by Toney et al. However, as pointed out in our previous paper, there is a discrepancy between the potential for adlayer rotation (≤ 160 mV vs Pb^{2+}/Pb)¹¹ and that where stress relaxation is observed (≈ 210 mV vs Pb^{2+}/Pb),^{12–14} indicating that there is no direct relationship between the relaxation and the rotation.

Several reports in the literature discuss the change in shape of the voltammetry for Pb upd on Au(111) as a function of sweep rate, particularly with respect to the shape of the double peak (at ca. -0.65 V vs SSE).^{11,15–17} The peak tends to become a clear double peak at fast sweep rates and a single peak at

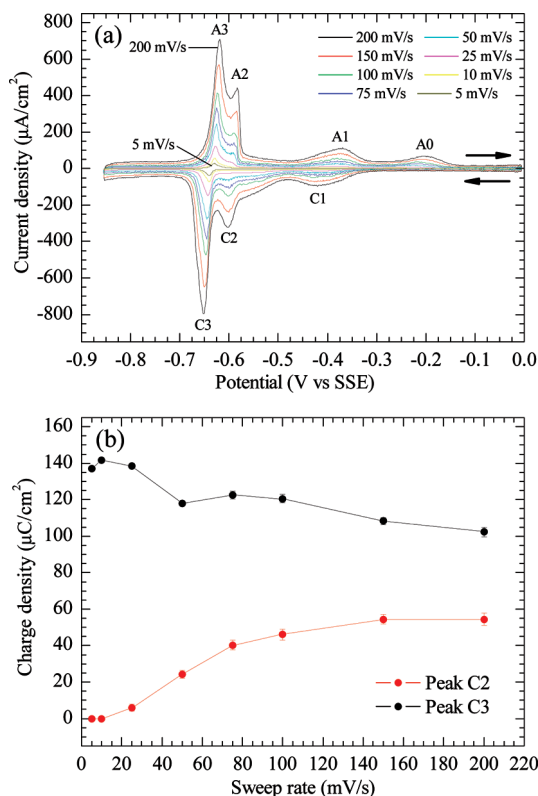


Figure 1. (a) Potentiodynamic scans at various sweep rates (5–200 mV/s) during Pb upd on (111)-textured Au film in 0.1 mol/L HClO_4 containing 10 mmol/L $\text{Pb}(\text{ClO}_4)_2$. (b) Plot of charge density vs potential sweep rate for peaks C2 and C3.

slow sweep rates as the peak at more positive potentials disappears, as shown in Figure 1a. Somewhat similar behavior has been observed in Pb and Tl upd on $\text{Ag}(111)$.^{18–21} Siegenthaler et al.^{18,19} have shown that the most pronounced upd peak (the second peak of the three upd peaks normally

* To whom correspondence should be addressed. E-mail: jaewook.shin@nist.gov. Phone: 301-975-6157. Fax: 301-926-7679.

observed) decreased and completely disappeared while the potential was cycled for an extended time within a narrow potential range around the second peak. Using scanning tunneling microscopy (STM),²² they found that the original hcp structure of the incomplete Pb adlayer was slowly transformed into the $(\sqrt{3}\times\sqrt{3})R30^\circ$ structure by exchanging every third Ag atom in the substrate with a Pb or Tl adsorbate atom during the extended cycling. In addition, they observed a new Pb deposition peak at a more cathodic potential, which was attributed to a cathodic shift of the Pb deposition potential on the surface alloy structure. Many researchers have failed to discuss surface alloying during Pb upd on Au(111) because the total charge agrees very well with the charge necessary for monolayer deposition of Pb on Au(111). Even after extended polarization at a fixed potential in the electrocompression region, the amount of charge measured during stripping was constant, regardless of polarization time, suggesting that no alloying is associated with the full monolayer. However, Green and Hanson have clearly shown STM evidence for surface alloying by both lateral and vertical atomic exchange, but the alloying is limited to low coverage of Pb on Au(111).²³ This suggests that the voltammetric peak shape change observed during Pb upd on Au(111) is associated with a surface structure change, similar to the case of Pb on Ag(111). It also indicates that a dealloying step is associated with completion of the Pb monolayer, similar to the cases of Pb or Bi on Cu(111) or Cu(100).^{24–26} This behavior is clearly different from systems, such as Cd/Ag(111), which alloy into the solid state at full coverage. In this case, the charge required to strip the Cd exceeds that of a monolayer and generally exhibits a $t^{1/2}$ dependence with alloying time.^{27,28}

We have also noticed that the stress relaxation hump is linked to the voltammetric peak shape change. The clearer the double peak, the smaller the magnitude of stress relaxation, whereas when a single peak is observed, the stress relaxation shows a maximum value. On the basis of these observations, we put forth the hypothesis that the stress relaxation hump is associated with surface alloying in the low-coverage region.

To better understand both the voltammetric and the surface stress response to the Pb upd processes, we have investigated these in more detail using highly textured Au(111) evaporated films. In addition, we have examined the steady-state surface stress response following long-term potential pulses from 0 V, where there is no Pb deposit on Au, to various potentials in the upd region, down to bulk Pb deposition. The results from these experiments reveal strong evidence for kinetically controlled surface alloying of Pb on Au(111), but only in the low-coverage region, and that the extent of surface alloy formation is strongly dependent on sweep rate. We also conclude that the complete monolayer of Pb is formed as a result of both a dealloying process and further Pb deposition and that the alloying/dealloying transition causes the stress relaxation hump.

Experimental Section

The surface stress was measured in situ on a (111)-textured Au film in the Pb upd region using the wafer curvature method. The substrate was a borosilicate glass strip (Schott) (certain trade names are mentioned for experimental information only; in no case does it imply a recommendation or endorsement by NIST) with dimensions of 60 mm \times 3 mm \times 108 μ m. The glass had a Young's modulus of 72.9×10^9 N/m² and a Poisson ratio of 0.208. Before evaporating Au, the glass substrate was cleaned in acetone for 30 min and dried by nitrogen gas. This was followed by reactive ion etching for 10 min. A 250 nm thick Au film was vapor-deposited at 0.1 nm/s after deposition of a

5 nm thick Ti adhesion layer. All sample preparation was performed in a clean room (class 100) to minimize contamination of the surface. The evaporated Au film showed a strong (111) texture. In θ - 2θ X-ray scans, no 200 reflection was observed and the rocking curve of the (111) reflection typically had a full width at half-maximum (fwhm) of $\approx 1.7^\circ$. The grain size was determined by field emission scanning electron microscopy to be on the order of 100 nm.

The electrochemical cell was a single-compartment Pyrex cell covered by a perfluorethylene cap. A platinum sheet was used as a counter electrode and a SSE was used as a reference electrode with a salt bridge filled with saturated K₂SO₄. The electrolyte was 0.1 mol/L HClO₄ (Sigma-Aldrich, 99.999%) containing 10 mmol/L Pb(ClO₄)₂ (Sigma-Aldrich, 99.999%). The electrolyte was prepared using 18.3 M Ω ·cm ultrapure water. Prior to use, the Au substrate was cleaned in piranha solution (3:1 volume mixture of concentrated H₂SO₄ and 30% H₂O₂) for approximately 5 s and was electrochemically cycled several times in the electrolyte between potentials for complete Pb monolayer deposition (-0.85 V/SSE) and Au oxide formation (1.0 V/SSE). The electrolyte was purged with pure nitrogen to remove the dissolved oxygen in the solution. A nitrogen purge was maintained in the head space during all measurements. The potential was controlled by an EG&G Princeton Applied Research Corp. (PARC) model 273 potentiostat–galvanostat, using a PC with LabView software. The usual data acquisition rate was 50 Hz for cyclic voltammetry, but the rate was increased to 100 Hz for the potentiostatic pulse experiments in order to capture the initial rapid changes in surface stress following the pulse. The curvature of the substrate was monitored while in solution and under potential control by reflecting a HeNe laser off of the glass/metal interface and onto a position-sensitive detector. The surface stress was calculated from Stoney's equation. Details of the experimental apparatus and procedures for the stress measurement are described elsewhere.^{29,30}

Results

Figure 1a shows potentiodynamic scans at various sweep rates during Pb upd on (111)-textured Au in 0.1 mol/L HClO₄ containing 10 mmol/L Pb(ClO₄)₂. The cyclic voltammeter is qualitatively identical to that which we reported in our previous study. However, certain voltammetric details, such as the double peaks (C2/C3 and A2/A3) and the irreversible anodic peak (A0) that have been observed in voltammetry using a Au(111) single crystal,^{31–34} are more pronounced because the Au film in these experiments has improved (111) texture (fwhm of $\approx 1.7^\circ$) compared with that of our previous study (fwhm of $\approx 3^\circ$). Hamelin showed that the double peak and the irreversible anodic peak are closely related to the presence of large (111) terraces by comparing voltammetry from single crystals with various misorientations.^{31,33} The first pair of peaks (C1/A1) is reported to be due to Pb adsorption/desorption at step edges.^{8,10,31} With further decreasing of potential, the nucleation and growth of hcp Pb islands were observed by STM^{8,9} and atomic force microscopy (AFM).¹⁰ At potentials more negative than the principal upd peak (C3), Pb islands coalesce and form a complete hcp monolayer that is incommensurate with respect to the Au(111). Using X-ray scattering, Toney et al.¹¹ have shown that the Pb adlayer rotates with respect to the Au(111) substrate in this potential region and that the Pb interatomic spacing decreases with decreasing potential.

Figure 1a shows that, at fast sweep rates, the double peaks (C2/C3, A2/A3) are clearly formed, but at slow sweep rates (5

and 10 mV/s), peak C2 disappears completely. This phenomenon is consistent with other investigators' observations.^{11,15–17} Figure 1b shows the plot of the charge density of the C2 and C3 peaks versus voltammetric sweep rate. As the sweep rate decreases, the charge associated with peak C3 increases while that associated with peak C2 decreases, eventually becoming 0 at 10 mV/s. This change in charge density suggests that there are subtle changes to the Pb upd process with varying sweep rates. The STM observation during Pb upd on Au(111)²³ supports this, showing that the surface structure changes over time at low Pb coverage. Specifically, when Pb was deposited with a coverage of ≈ 0.25 ML, Pb islands of monolayer height were initially observed. However, a second phase, with a $(\sqrt{3} \times \sqrt{3})$ R30° structure, appeared and slowly filled the terrace spaces between the Pb islands, while the potential was held constant. This phase transformation is only observed at low Pb coverage and has not been observed for the complete monolayer. According to this observation, the surface alloy phase will cover more of the Au(111) surface as the potential remains within the low-coverage range. In addition, the Pb deposition potential shifts to more negative values for deposition on the alloy structure, as observed during Pb upd on Ag(111) after extended cyclic polarization.¹⁹ Considering these facts, a significant portion of the Au(111) surface would be transformed to the surface alloy structure at slow sweep rates, thereby preventing further deposition of Pb at the potential of peak C2 where the deposition of the hcp Pb adlayer on the unalloyed Au(111) surface should occur. As a consequence, peak C2 is reduced and finally disappears at slow sweep rates. However, at fast sweep rates, more of the Au(111) surface would be alloy-free so that Pb deposition can occur on these terraces, giving rise to peak C2. Peak C3 is associated with completion of the Pb monolayer and also appears to be dependent on the extent of surface alloying (or sweep rate). We conclude that a dealloying process is required in order for the Pb coverage to increase to full coverage. This dealloying process will be discussed later along with the surface stress behavior.

Figure 2a shows the change in surface stress during cyclic voltammetry in 0.1 mol/L HClO₄ with and without Pb²⁺ at various sweep rates (5–200 mV/s). Without Pb²⁺, the surface stress increases due to a combination of electrocapillarity and surface charge redistribution induced by anion desorption during the cathodic scan.³⁵ The Pb²⁺-free surface stress does not show any sweep rate dependence, so only the curve scanned at 100 mV/s is shown. The potentiodynamic scan was stopped at -0.6 V because hydrogen started to evolve from the Au surface. With Pb²⁺ in the electrolyte, the surface stress initially showed the same tensile increase during the cathodic sweeps; however, at a potential of about -0.43 V, it begins to deviate in the compressive direction due to the nucleation and growth of Pb islands. The compressive stress continues until stress relaxation in the tensile direction occurs in a very narrow potential range (-0.635 to -0.670 V), after which the Pb monolayer is completed. With further deposition, the stress once again moves in the compressive direction as more Pb atoms are incorporated into the adlayer, causing contraction of the interatomic spacing and eventually rotation of the monolayer. Hydrogen evolution on the Pb adlayer is suppressed down to about -0.85 V. During the anodic sweeps, the surface stress shows reversible behavior within the electrocompression region; however, following the stress hump, large hysteresis is observed, with the anodic sweep showing more compressive stress than the corresponding cathodic sweep. When the potential reached 0 V, the surface stress returned to its initial value, indicating that all of the Pb

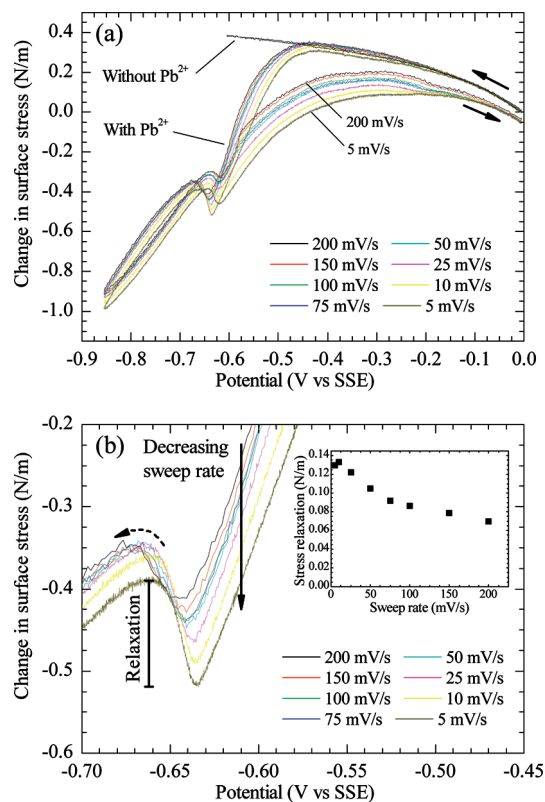


Figure 2. (a) Change in surface stress during Pb upd on (111)-textured Au film at various sweep rates (5–200 mV/s) in 0.1 mol/L HClO₄ with and without 10 mmol/L Pb(ClO₄)₂. (b) The change in surface stress is magnified around the potential range of the stress relaxation. Only cathodic scans are shown. The inset shows the magnitude of stress relaxation during cathodic scans as a function of sweep rate.

had been stripped from the Au surface. The sweep rate dependence of surface stress is clearly shown in Figure 2b. Although the surface stress was arbitrarily defined to be zero at the start of each scan (at 0 V), larger compressive stress clearly developed when the potential was scanned at slower sweep rates. This stress behavior can be explained within the same framework of the surface alloying processes discussed above.

Surface stresses arise because the atomic configuration of atoms at a surface is different than that in the bulk. Ibach³⁶ has suggested that the loss of bonds at a clean metal surface causes an increased charge density between the remaining surface atoms, thereby increasing their attractive interaction and resulting in a tensile stress at the surface. This tensile stress, which has been calculated to be 2.77 N/m for Au(111),³⁷ has been observed in most free-electron metals and is a likely driving force for surface reconstruction³⁶ as well as surface alloying between large adsorbates and smaller substrate atoms. Such surface alloying has recently been supported by density functional theory (DFT)³⁸ and effective medium theory (EMT)³⁹ calculations. Self-assembly of surface alloy domains has also been attributed to surface stress.⁴⁰ In Pb upd on Au(111), the hcp adlayer is slowly transformed to the surface alloy because the alloy structure is more stable than the hcp structure at low Pb coverage. The phase transformation is accompanied by an additional compressive shift in the surface stress. This explains the larger compressive stress that is observed when the potential was scanned at slower sweep rates; that is, the slow sweep rate allows more time for the hcp adlayer to transform to the alloy structure. The stress relaxation hump also shows the same tendency. As shown in the inset of Figure 2b, the magnitude of stress relaxation was larger at slower sweep rates. In other words, the more heavily

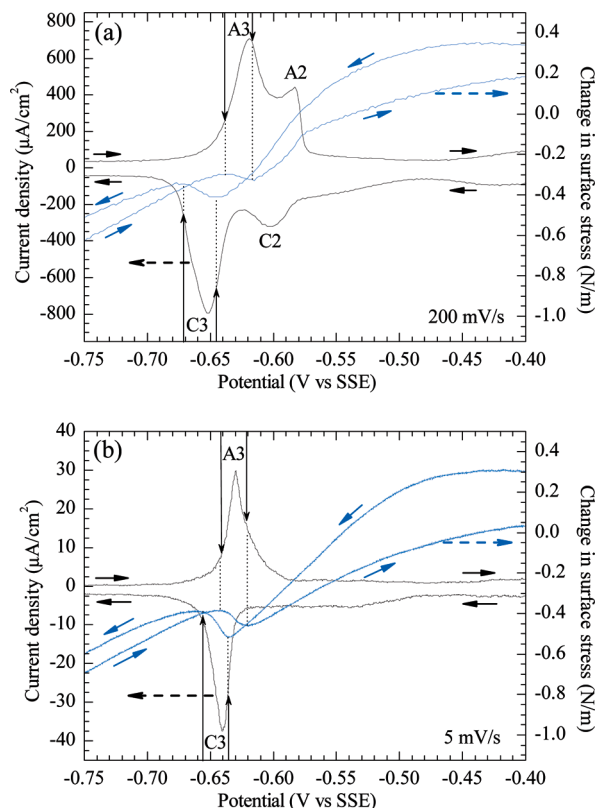


Figure 3. Potentiodynamic scan and change in surface stress during Pb upd on (111)-textured Au film in 0.1 mol/L HClO₄ containing 10 mmol/L Pb(ClO₄)₂ at a sweep rate of (a) 200 and (b) 5 mV/s.

alloyed surface (slower sweep rate) caused more tensile relaxation, whereas the less alloyed surface (faster sweep rate) caused less tensile relaxation during completion of the Pb monolayer. This stress relaxation behavior must be related to the interaction between the alloy structure and the additional Pb deposit. At low coverage, when the Au(111) surface between the hcp Pb islands is filled with the alloyed structure during cathodic scans, the Pb coverage can be further increased in three ways: increase the Pb content of the alloy, form hcp islands of Pb on top of the alloy, or restructure the surface so that islands of hcp Pb form directly on the Au(111) surface. Starting with the first scenario, there is a limit to how much Pb the Au layer can accept. EMT calculations for Au on Ni (110) clearly show that the energy of the alloy increases with solute (Au) concentration.³⁹ At some concentration, the monatomic adlayer will be thermodynamically more stable than the alloy. At that point, new islands of Pb can form on the alloy; however, there seems to be a positive interface energy between the Pb adlayer and the alloyed surface. This positive interface energy can be deduced by Schmidt et al.'s observation,¹⁹ in which a more negative potential was required to deposit Pb on the Pb–Ag alloyed structure. That leaves the final option: to achieve high coverage, the alloy must reverse transform so that the hcp Pb monolayer forms on the unalloyed Au surface. Therefore, it is reasonable to conclude that a complete Pb layer is formed by a dealloying process and stress relaxation in the tensile direction is a consequence of this process. There are also other cases that support the dealloying of a surface alloy at high coverage. For example, the dealloying of Pb on Cu(111)²⁴ and Bi on Cu(100)^{25,26} have been observed by surface X-ray diffraction (SXRD) and low-energy electron diffraction (LEED).

The surface alloying at low coverage is observed again during the anodic sweeps. Figure 3 shows the cyclic voltammetry with

corresponding surface stress at a fast sweep rate (panel a, 200 mV/s) and a slow sweep rate (panel b, 5 mV/s). As the potential increases from the cathodic end, the compressive stress in the continuous Pb monolayer decreases up to peak A3 because Pb atoms are removed from the adlayer. Within the narrow potential range around peak A3, as indicated by vertical arrows, the monolayer breaks up into discrete islands and compressive stress increases. This is not surprising because the surface alloy structure is thermodynamically more stable than the hcp structure in the submonolayer regime. As soon as the monolayer turns into discrete Pb islands, the surface alloying process will proceed again, creating compressive stress. When the potential approaches peak A2, the Pb islands that retained the hcp structure are dissolved first. During this relatively fast dissolution process, the surface stress resumes its trend toward more tensile values with increasing potential. The subsequent dissolution of the remaining surface alloy structure is a slower process, so the rate of tensile stress development is decreased at potentials more positive than -0.58 V, as seen in Figure 3a. The transition between fast and slow dissolution depends on the extent of surface alloying during the anodic sweeps. Once the continuous monolayer is broken, more surface alloy formation is expected at slower sweep rates. When the peak A2 potential is reached, very little of the Pb that remains on the surface is unalloyed and able to be dissolved at this potential. Indeed, no current peak is observed at the potential of peak A2 at 5 mV/s, as shown in Figure 3b. The corresponding surface stress shows a slow and monotonic decrease of compressive stress, without the tensile jump associated with peak A2. As a consequence, the slow sweep rate stress response shows a larger hysteresis in the compressive direction than that of the fast sweep rate. This indicates that, at the slow sweep rate, most of the Pb atoms were already transformed into the alloy structure before they were oxidized back into solution.

Because the alloying is a slow process, long-term potentiostatic pulse experiments can provide useful information about the kinetics and the equilibrium state as a function of potential. Figure 4 shows the change in surface stress during the potentiostatic pulse experiments. In each experiment, the potential was initially held at 0 V until the surface stress had stabilized. Background data were collected for 20 s, and then the potential was stepped to various values between -0.100 and -0.850 V and was maintained for 40 s. Afterward, the potential was stepped back to 0 V, and the stress was measured for an additional 60 s. Figure 4a shows the stress changes with potential steps between -0.100 and -0.450 V where the stress change by electrocapillarity and anion desorption is dominant. As expected from the stress change observed during the potentiodynamic scans, larger tensile stress was measured with a more negative potential step. The response of the surface stress was immediate after the potential step, indicating that anion adsorption/desorption is a relatively fast process.

Figure 4b shows the stress response for potential steps between -0.475 and -0.630 V, where low-coverage Pb deposition is expected. The surface stress first jumped to the tensile value indicative of anion desorption before rapidly settling to a more negative value that depended on the Pb coverage at that particular potential. The surface stress then became more compressive for the duration of the 40 s pulse. In this potential range, the Pb adlayer is submonolayer, and the hcp Pb islands that initially form slowly transform to the surface alloy structure. The development of compressive stress with time following the potential pulse strongly supports the slow phase transformation at low coverage of Pb on Au(111). It is

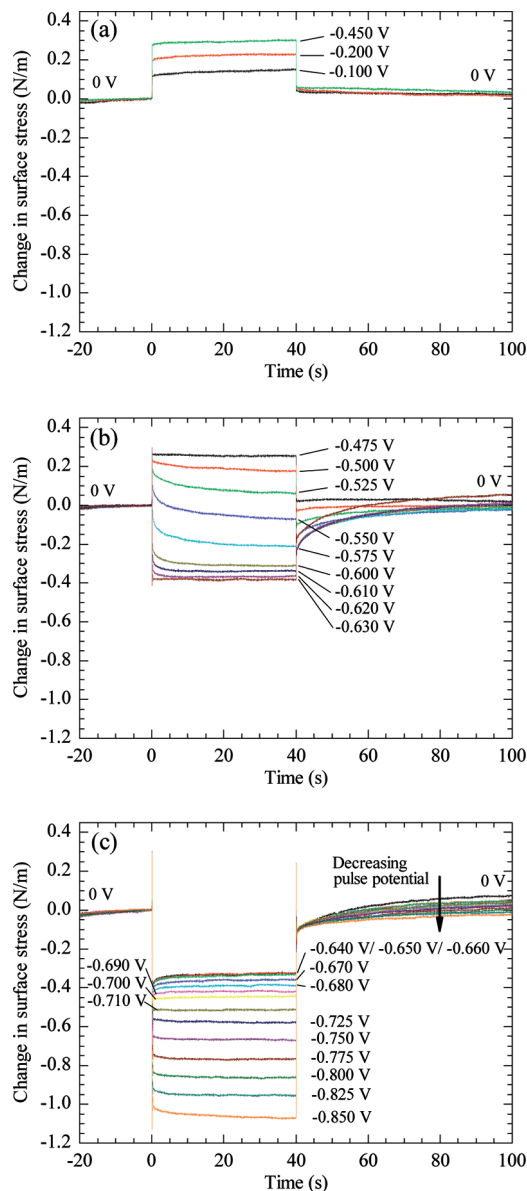


Figure 4. Change in surface stress during long-term potentiostatic pulses from 0 V to various potentials: (a) -0.100 to -0.450 , (b) -0.475 to -0.630 , (c) -0.640 to -0.850 V.

interesting to note the -0.475 V transient. At this potential, a small amount of Pb is deposited, presumably, at step edges. In this case, surface alloying by lateral exchange of atoms is expected. The surface stress after the potential step was slightly more compressive than that of the previous step at -0.450 V due to the higher Pb coverage. However, even with the apparent alloying, the stress value was essentially constant for the entire pulse. Further, when the potential was stepped back to 0 V, the stress immediately recovered to zero stress. This suggests that the lateral exchange process is very fast compared with the vertical exchange process and that the compressive stress associated with this process is rather small. As the potential step is made more negative, the compressive stress transient during the potential hold becomes larger, showing a maximum change at -0.575 V, and then finally diminishes again at -0.630 V. All of the stress transients that generated compressive stress during the cathodic pulse also showed a sluggish response in the tensile direction as the Pb was stripped from the Au surface. This behavior can be understood by the competing processes of hcp Pb island deposition and surface alloying. Green and

Hanson observed that the alloy phase, over time at a fixed potential, filled the space between the Pb islands.²³ This suggests that the exposed Au(111) surface is a necessary condition for growth of the surface alloy. At more positive potentials, the Pb coverage is small, so there would be appreciable space between the Pb islands for alloy formation. As a consequence, a large compressive stress transient is observed. However, at more negative potentials, the hcp Pb coverage is high. The interisland spaces are small and would be filled with the surface alloy more quickly, thereby inducing less compressive stress. At -0.630 V, the surface stress remained constant after the potential pulse, indicating that no surface alloying had occurred during the potential hold period. This does not mean that the entire surface was covered by the hcp Pb monolayer because the stripping pulse showed a clear signature of alloying (slow recovery of stress). This simply implies that some alloying occurs almost immediately during the potential step. Green and Hanson also showed that the Pb is preferentially deposited on defect sites on terraces, such as vacancies. A surface alloy could be formed immediately after the potential pulse around those defect sites. The fact that the stress hump is also observed at very fast sweep rates supports the idea of very fast surface alloying at some defect sites.

The potential between -0.640 and -0.660 V is the range where peak C3 appears during the cathodic potentiodynamic scans. As seen in Figure 4c, the stress values measured directly following the potential pulses fall into a very narrow range. This is in spite of the significantly increased Pb coverage as a result of peak C3, which might be expected to induce compressive stress. Furthermore, not only is the compressive stress less than expected, based on Pb coverage, but the stress relaxes in the tensile direction following the potential step. This suggests that the entire surface is already covered by the mixture of surface alloy and hcp Pb islands when the potential is pulsed to -0.630 V. When the potential is pulsed to more negative potentials, the only way to increase the Pb coverage is by transforming some of the less dense surface alloy structure to a denser hcp structure by dealloying and depositing additional Pb. The development of tensile stress in the early stages of the potential hold reflects the dealloying process at high coverage. When the potential was pulsed back to 0 V, the stress recovered to the initial value fairly quickly, suggesting that little dealloying had occurred during this stripping step. We can also conclude that the amount of remaining surface alloy in the adlayer decreased as the potential was pulsed to more negative values, based on the observation that the surface stress after stripping showed less change while the potential was held at 0 V (indicated by an arrow in Figure 4c). When the potential is stepped to values more negative than that of peak C3, the formation of a full monolayer of Pb is expected. As seen in Figure 4c, the stress is fairly constant for pulse potentials more negative than -0.70 V, indicating that no structural change takes place on the surface during the potential hold. In this potential range, the compressive stress following each pulse increased with more negative potential as the incommensurate hcp Pb adlayer was elastically compressed by the insertion of additional Pb atoms into the layer.

It is also interesting to note in Figure 4c the sequential nature of the stress response to the potential step. For example, when the potential is stepped from 0 V down to -0.85 V, what appears to be a stress spike up to $+0.30$ N/m is the stress response associated with electrocapillarity and anion desorption. The stress transient captures all stages of the deposition process, not just that of the final adlayer. The same is true for the stripping pulse. The stress spike of $+0.25$ N/m following the potential

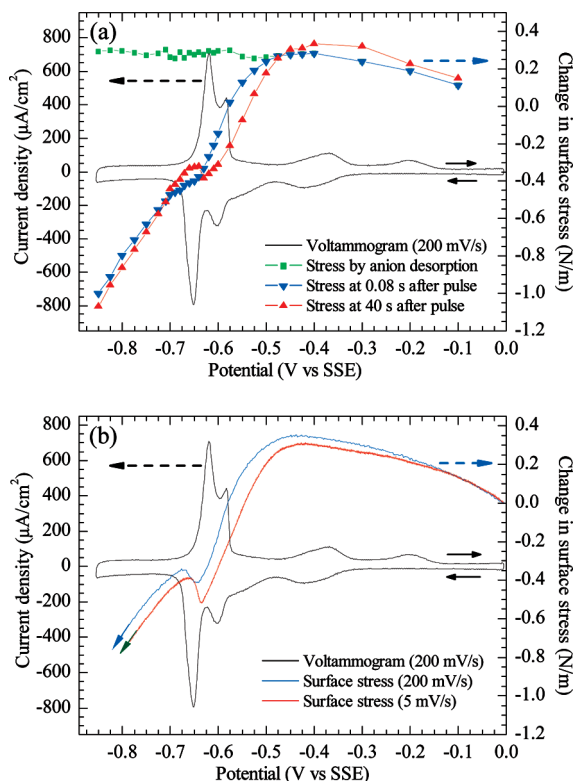


Figure 5. (a) Surface stress response during the potentiostatic pulses in Figure 4 that were obtained at the tensile spikes right after the pulses (■) and at 0.08 s (▼) and at 40 s (▲) after the pulses. The stress values were plotted as a function of potential with a voltammogram at a scan rate of 200 mV/s. (b) Changes in surface stress for potentiodynamic scans of 200 and 5 mV/s (for cathodic scan only) plotted with a voltammogram at a scan rate of 200 mV/s.

step back to 0.0 V captures the stripping of the hcp Pb, the electrocapillarity associated with the potential change, and the readsorption of perchlorate onto the Au surface. These are very fast processes. It is only the dealloying step that requires additional time for the stress to stabilize, reflecting the time constant of the process.

The results of the long-term potentiostatic pulse experiments are summarized in Figure 5a. The squares (■) represent the stress change due to anion desorption following each potential pulse. These values were taken from the tensile spikes at 0 s in Figure 4b,c, which show the clear sequential process of tensile stress from anion desorption, followed by compressive stress from Pb upd. The reverse triangles (▼) and the triangles (▲) represent the surface stress at 0.08 and 40 s into the potentiostatic pulses, respectively. The compressive transients by surface alloying are observed between -0.475 and -0.630 V, and the tensile transients by dealloying are observed between -0.640 and -0.700 V as vertical gaps between the triangles and the reverse triangles. The two curves are essentially identical in the compression region, negative of -0.70 V.

The general shape and the values of stress during the potentiostatic pulses are very similar to those of the potentiodynamic scans, as shown in Figure 5b. The values of surface stress immediately after the potentiostatic pulses are well-matched to those of the fastest sweep rate (200 mV/s). Similarly, the values of surface stress recorded 40 s after the potentiostatic pulses are close to those of the slowest sweep rate (5 mV/s). The similarity of changes in surface stress observed in the sweep rate dependence during the potentiodynamic scans and stress transients during the potentiostatic pulses is due to the relation

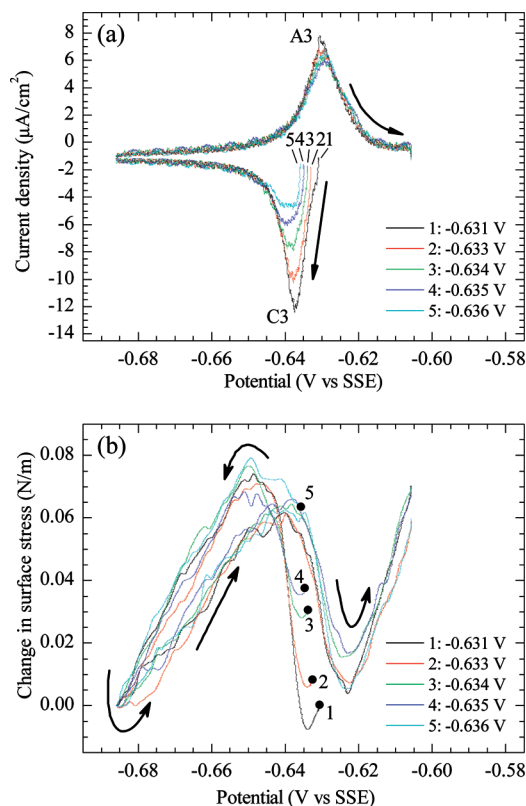


Figure 6. (a) Potentiodynamic scans starting from various potentials following a 1 min hold. (b) The change in surface stress corresponding to the potentiodynamic scans. The stress values at -0.685 V for all scans were matched to zero stress.

between surface stress and surface alloying. When there is little surface alloying, which is the case for 200 mV/s and 0.08 s into the pulse, the development of compressive stress is small. However, when there is significant surface alloying, which is the case for 5 mV/s and 40 s into the pulse, more compressive stress develops.

In the potential region of peak C3, the stress relaxation is observed during both the potentiostatic pulses and the potentiodynamic scans. However, the stress relaxation hump observed from the potentiostatic pulses is much weaker than that from the potentiodynamic scans. This is most likely due to the fact that the potentiodynamic scan causes a gradual increase in the Pb coverage, whereas the potentiostatic pulse causes an instantaneous increase in coverage. The gradual increase in the coverage will cause more compressive stress to develop due to the formation of the surface alloy during the cathodic scan.

To gain a better understanding of the surface structure within the narrow potential range for the stress relaxation hump, the cyclic voltammetry and the corresponding change in surface stress were measured after the potential was held at a constant value, ranging between -0.631 and -0.636 V, for about 1 min in order to stabilize the surface structure at each potential. As shown in Figure 6a, the potential was first scanned cathodically down to -0.685 V and then scanned anodically up to -0.605 V at 1 mV/s. Peak C3 became smaller when the scan started at more negative potential, whereas the stripping peak A3 was essentially the same. This indicates that the Pb coverage at the starting point was higher when the potential was maintained at a more negative potential. The reduced peak height of C3 indicates that less material was required to complete the monolayer.

The corresponding changes in surface stress for these voltammograms are shown in Figure 6b. In this case, the fully

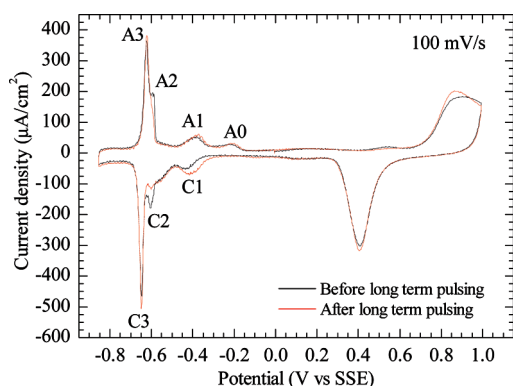


Figure 7. Potentiodynamic scans of Pb upd on (111)-textured Au in 0.1 mol/L HClO_4 with 10 mmol/L $\text{Pb}(\text{ClO}_4)_2$ before and after the long-term potentiostatic pulse experiments.

compressed monolayer at -0.685 V was arbitrarily chosen as the reference (zero) stress state. Stress relaxation in the tensile direction was observed during the cathodic scan in all of the cyclic scans, the magnitude of which decreased with the more negative starting potential. The stress relaxation indicates that the alloy structure is stable even after the potential was maintained for a long period of time. However, the fact that the magnitude of the stress relaxation decreases indicates that the amount of alloy decreases as the starting potential is made more negative; that is, more of the alloy structure reverse transforms to the hcp structure during the potential hold.

In Figure 7, the voltammograms before and after the long-term pulsing experiments are compared. The anodic peak at $+0.9$ V and the cathodic peak at $+0.4$ V are due to Au oxide formation and reduction, respectively. The black curve is that of a new Au cantilever electrode, whereas the red curve is that of the Au after many surface alloying and dealloying cycles. After the long-term pulsing experiments, peaks C1/A1 and C3/A3 became somewhat larger while peaks C2/A2 became smaller. The increase of peak C1/A1 implies that Pb adsorption at step edges and defect sites increased. The decrease of peaks C2/A2 can be interpreted as the reduction of the Au(111) area for hcp Pb deposition between alloyed areas due to the fast formation of surface alloys around defect sites. As a result of the decrease in peaks C2/A2, peaks C3/A3 become larger because a larger amount of surface alloy is transformed into the hcp structure. In addition, the roughness factor of the (111)-textured Au surface increased after the long-term pulsing experiments, as seen from the increased area of the Au oxide reduction peak at 0.4 V. The changes in the voltammetry before and after the pulsing experiments are consistent with the consequence of roughening by surface alloying and dealloying.

Conclusion

We examined the voltammetry and surface stress during Pb upd on (111)-textured Au in perchloric acid supporting electrolyte. The sweep rate dependence in peak height and the stress relaxation hump at the transition between submonolayer to monolayer were interpreted as the result of kinetically controlled surface alloying and dealloying processes. At slower sweep rates, a larger portion of the surface is transformed to the alloy structure because more time is given for phase transformation. The decrease of the cathodic peak at -0.6 V (C2) at slower sweep rates is related to the small area of alloy-free Au(111) that exists between the alloyed areas and is available for hcp Pb deposition. The larger stress relaxation at slower sweep rates is the result of dealloying the large area of the surface alloy that forms over the extended time. The surface

alloying and dealloying process is also confirmed by the long-term pulsing experiments, which showed the slow stress changes during both deposition pulses and dissolution pulses, within the potential range where surface alloying is expected. When the surface of Au(111) is covered with the mixture of hcp and the alloy structure of Pb, the alloy structure is stable even after the potential is maintained for an extended time. The relative amount of hcp Pb and the alloy structure is a function of potential. After many cycles of Pb deposition and dissolution, the (111)-textured Au surface is roughened, as a consequence of surface alloying and dealloying processes.

Acknowledgment. This work was performed, in part, at the Center for Nanoscale Science and Technology NanoFab at the National Institute of Standards and Technology.

References and Notes

- (1) Alvarez, M.; Jüttner, K. *J. Electroanal. Chem.* **1983**, *144*, 351.
- (2) Jüttner, K. *Electrochim. Acta* **1986**, *31*, 917.
- (3) Alvarez, M.; Jüttner, K. *Electrochim. Acta* **1988**, *33*, 33.
- (4) Hsieh, S.-J.; Gewirth, A. A. *Surf. Sci.* **2002**, *498*, 147.
- (5) Pauling, H. J.; Jüttner, K. *Electrochim. Acta* **1992**, *37*, 2237.
- (6) Pauling, H. J.; Staikov, G.; Jüttner, K. *J. Electroanal. Chem.* **1994**, *376*, 179.
- (7) Lorenz, W. J.; Staikov, G. *Surf. Sci.* **1995**, *335*, 32.
- (8) Green, M. P.; Hanson, K. J.; Carr, R.; Lindau, I. *J. Electrochem. Soc.* **1990**, *137*, 3493.
- (9) Tao, N. J.; Pan, J.; Li, Y.; Oden, P. I.; DeRose, J. A.; Lindsay, S. M. *Surf. Sci.* **1992**, *271*, L338.
- (10) Chen, C.-H.; Washburn, N.; Gewirth, A. A. *J. Phys. Chem.* **1993**, *97*, 9754.
- (11) Toney, M. F.; Gordon, J. G.; Samant, M. G.; Borges, G. L.; Melroy, O. R.; Yee, D.; Sorensen, L. B. *J. Phys. Chem.* **1995**, *99*, 4733.
- (12) Stafford, G. R.; Bertocci, U. *J. Phys. Chem. C* **2007**, *111*, 17580.
- (13) Seo, M.; Yamazaki, M. *J. Electrochem. Soc.* **2004**, *151*, E276.
- (14) Friesen, C.; Dimitrov, N.; Cammarata, R. C.; Sieradzki, K. *Langmuir* **2001**, *17*, 807.
- (15) Adzic, R.; Yeager, E.; Cahan, B. D. *J. Electrochem. Soc.* **1974**, *121*, 474.
- (16) Schultze, J. W.; Dickertmann, D. *Surf. Sci.* **1976**, *54*, 489.
- (17) Brunt, T. A.; Rayment, T.; O'Shea, S. J.; Welland, M. E. *Langmuir* **1996**, *12*, 5942.
- (18) Siegenthaler, H.; Jüttner, K. *Electrochim. Acta* **1979**, *24*, 109.
- (19) Schmidt, E.; Siegenthaler, H. *J. Electroanal. Chem.* **1983**, *150*, 59.
- (20) Popov, A.; Dimitrov, N.; Velez, O.; Vitanov, T.; Budevski, E. *Electrochim. Acta* **1989**, *34*, 265.
- (21) Dimitrov, N.; Popov, A.; Vitanov, T.; Budevski, E. *Electrochim. Acta* **1991**, *36*, 2077.
- (22) Carnal, D.; Oden, P. I.; Müller, U.; Schmidt, E.; Siegenthaler, H. *Electrochim. Acta* **1995**, *40*, 1223.
- (23) Green, M. P.; Hanson, K. J. *Surf. Sci.* **1991**, *259*, L743.
- (24) Nagl, C.; Haller, O.; Platzgummer, E.; Schmid, M.; Varga, P. *Surf. Sci.* **1994**, *321*, 237.
- (25) Meyerheim, H. L.; Zajonz, H.; Moritz, W.; Robinson, I. K. *Surf. Sci.* **1997**, *381*, L551.
- (26) AlShamaileh, E.; Barnes, C. *Phys. Chem. Chem. Phys.* **2002**, *4*, 5148.
- (27) Bort, H.; Jüttner, K.; Lorenz, W. J.; Staikov, G. *Electrochim. Acta* **1983**, *28*, 993.
- (28) García, S. G.; Salinas, D. R.; Staikov, G. *Surf. Sci.* **2005**, *576*, 9.
- (29) Kongstein, O. E.; Bertocci, U.; Stafford, G. R. *J. Electrochem. Soc.* **2005**, *152*, C116.
- (30) Stafford, G. R.; Bertocci, U. *J. Phys. Chem. B* **2006**, *110*, 15493.
- (31) Hamelin, A. *J. Electroanal. Chem.* **1979**, *101*, 285.
- (32) Engelsmann, K.; Lorenz, W. J. *J. Electroanal. Chem.* **1980**, *114*, 1.
- (33) Hamelin, A. *J. Electroanal. Chem.* **1984**, *165*, 167.
- (34) Hamelin, A.; Lipkowski, J. *J. Electroanal. Chem.* **1984**, *171*, 317.
- (35) Ibach, H. *J. Vac. Sci. Technol., A* **1994**, *12*, 2240.
- (36) Ibach, H. *Surf. Sci. Rep.* **1997**, *29*, 193.
- (37) Payne, M. C.; Roberts, N.; Needs, R. J.; Needels, M.; Joannopoulos, J. D. *Surf. Sci.* **1989**, *211*, 1.
- (38) Harrison, M. J.; Woodruff, D. P.; Robinson, J. *Surf. Sci.* **2004**, *572*, 309.
- (39) Nielsen, L.; Besenbacher, F.; Stensgaard, I.; Lægsgaard, E. *Phys. Rev. Lett.* **1995**, *74*, 1159.
- (40) Kukta, R. V.; Vasiljevic, N.; Dimitrov, N.; Sieradzki, K. *Phys. Rev. Lett.* **2005**, *95*, 186103.